ELectronics EXpress

LETTER

IEICE Electronics Express, Vol.15, No.23, 1–12

Single-phase three-level grid-connected inverter based on direct adaptive fuzzy control

Xiaogang Wang[a)] **and Jingyu Yang**

College of Mechanical and Electrical Engineering, Guangzhou University, 230 Waihuan Xi Road, Guangzhou 510006, China

a) wxg@gzhu.edu.cn

Abstract: Single-phase three-level grid-connected inverter is widely used in high-voltage applications, which can be connected to the grid through a single inductor (L filter) or an LCL filter. The control schemes for an LCL-based grid-connected inverter are more complex than those for an L-based one to damp the resonance of the LCL filter. In this paper, a robust nonlinear direct adaptive fuzzy control scheme is proposed to control both the L- and LCL-based inverters. The principle of the inverter is introduced, especially the space vector pulse width modulation method for the single-phase three-level inverters. Then, the theory of the direct adaptive fuzzy control is described. Based on the theory, the current controller for both types of grid-connected inverters is designed. The closed-loop stability is proved based on the Lyapunov theory. Finally, simulations are conducted to verify the effectiveness of the controller. The results show that both the L- and LCL-based grid-connected inverters operate well with strong robustness under the same controller.

Keywords: three-level, adaptive fuzzy control, grid-connected inverter, stability

Classification: Power devices and circuits

References

[1] V. Yaramasu, *et al.*: "Predictive control for low-voltage ride-through enhancement of three-level-boost and NPC-converter based PMSG wind turbine," IEEE Trans. Ind. Electron. **61** (2014) 6832 (DOI: 10.1109/TIE.2014.2314060).

[2] S. Wang, *et al.*: "Hybrid single-carrier-based pulse width modulation scheme for single-phase three-level neutral-point-clamped grid-side converters in electric railway traction," IET Power Electron. **9** (2016) 2500 (DOI: 10.1049/iet-pel.2015.0656).

[3] R. Maheshwari, *et al.*: "Design of neutral-point voltage controller of a three-level NPC inverter with small DC-link capacitors," IEEE Trans. Ind. Electron. **60** (2013) 1861 (DOI: 10.1109/TIE.2012.2202352).

[4] A. K. Balasubramanian, *et al.*: "Analysis and design of split-capacitor resistive inductive passive damping for LCL filters in grid-connected inverters," IET Power Electron. **6** (2013) 1822 (DOI: 10.1049/iet-pel.2012.0679).

[5] W. Wu, *et al.*: "A new design method for the passive damped LCL and LLCL filter-based single-phase grid-tied inverter," IEEE Trans. Ind. Electron. **60** (2013) 4339 (DOI: 10.1109/TIE.2012.2217725).

DOI: 10.1587/elex.15.20180838
Received September 3, 2018
Accepted November 6, 2018
Publicized November 16, 2018
Copyedited December 10, 2018

[6] D. Pan, *et al.*: "Capacitor-current-feedback active damping with reduced computation delay for improving robustness of LCL-type grid-connected inverter," IEEE Trans. Power Electron. **29** (2014) 3414 (DOI: 10.1109/TPEL.2013.2279206).
[7] M. B. Saïd-Romdhane, *et al.*: "Robust active damping methods for LCL filter-based grid-connected converters," IEEE Trans. Power Electron. **32** (2017) 6739 (DOI: 10.1109/TPEL.2016.2626290).
[8] M. Hanif, *et al.*: "Two degrees of freedom active damping technique for LCL filter-based grid connected PV systems," IEEE Trans. Ind. Electron. **61** (2014) 2795 (DOI: 10.1109/TIE.2013.2274416).
[9] J. Xu, *et al.*: "Active damping-based control for grid-connected LCL-filtered inverter with injected grid current feedback only," IEEE Trans. Ind. Electron. **61** (2014) 4746 (DOI: 10.1109/TIE.2013.2290771).
[10] L. Wang: "Stable adaptive fuzzy control of nonlinear systems," IEEE Trans. Fuzzy Syst. **1** (1993) 146 (DOI: 10.1109/91.227383).
[11] S. Tong, *et al.*: "Fuzzy adaptive output tracking control of nonlinear systems," Fuzzy Sets Syst. **111** (2000) 169 (DOI: 10.1016/S0165-0114(98)00058-X).
[12] S. Tong, *et al.*: "Direct adaptive fuzzy output tracking control of nonlinear systems," Fuzzy Sets Syst. **128** (2002) 107 (DOI: 10.1016/S0165-0114(01)00058-6).
[13] H.-X. Li, *et al.*: "A hybrid adaptive fuzzy control for a class of nonlinear MIMO systems," IEEE Trans. Fuzzy Syst. **11** (2003) 24 (DOI: 10.1109/TFUZZ.2002.806314).
[14] Y.-C. Hsueh, *et al.*: "Decomposed fuzzy systems and their application in direct adaptive fuzzy control," IEEE Trans. Cybern. **44** (2014) 1772 (DOI: 10.1109/TCYB.2013.2295114).
[15] Q. Zhou, *et al.*: "Adaptive output-feedback fuzzy tracking control for a class of nonlinear systems," IEEE Trans. Fuzzy Syst. **19** (2011) 972 (DOI: 10.1109/TFUZZ.2011.2158652).
[16] S. Fahas, *et al.*: "Fuzzy direct adaptive direct torque control of switched reluctance motors," Proc. 42nd Annual Conference of the IEEE Industrial Electronics Society (2016) 2809 (DOI: 10.1109/IECON.2016.7793942).
[17] K.-C. Liu, *et al.*: "Modeling, analysis, and robust adaptive fuzzy control for a class of switching power converters," Proc. 12th IEEE Conference on Industrial Electronics and Applications (2017) 1149 (DOI: 10.1109/ICIEA.2017.8283013).
[18] C. Zhou, *et al.*: "An improved direct adaptive fuzzy controller of an uncertain PMSM for web-based E-service systems," IEEE Trans. Fuzzy Syst. **23** (2015) 58 (DOI: 10.1109/TFUZZ.2014.2315675).

1 Introduction

Three-level neutral-point-clamped (NPC) inverters are widely used in high voltage and high power applications due to the low voltage stress of switching devices, the low output harmonics and the low operating frequency [1, 2, 3]. The NPC inverter can be connected to the grid through an L or an LCL filter to filter out the harmonics and to make the current controllable. The stabilization of the LCL filter requires some care to suppress its resonance, so the control stategies for an LCL-based grid-connected inverter are different from those for an L-based one. The passive damping solution consists in introducing a resistor, in parallel to one of the inductors or the capacitor [4, 5]. However, this reduces the filter's efficiency and

DOI: 10.1587/elex.15.20180838
Received September 3, 2018
Accepted November 6, 2018
Publicized November 16, 2018
Copyedited December 10, 2018

quality factor. In order to avoid these drawbacks, many active damping solutions have been proposed, which damp the resonance by using control schemes. One of the most popular approaches is based on state variable feedback. The capacitor current feedback achieves best damping effect, but meanwhile, the phase margin is reduced too [6, 7]. The grid-connected current derivative feedback can also damp the resonance, while the differential will cause the problem of noise amplification. Another approach uses notch filter to weaken the resonance peak [8, 9]. However, the precondition is that the resonant frequency of the LCL filter must be known exactly. The effectiveness will be lowered during application, which is caused by parameter drifts of the LCL filter. In summary, the existing control methods have poor adaptability and robustness, which cannot regulate both types of grid-connected inverters and the control performance will deteriorate under parameter variations.

Stable adaptive fuzzy control is proposed by Wang [10] and developed by Tong et al. [11, 12, 13, 14, 15] to control the nonlinear systems, which does not require an accurate mathematical model of the system under control. The stable nonlinear adaptive fuzzy control consists of two types of schemes: direct control and indirect control. If the fuzzy logic system is used as the controller, the control is called direct adaptive fuzzy control. If the fuzzy logic system is used to model the controlled object, then the control is named as indirect adaptive fuzzy control. The distinguishing features of this fuzzy control method are the Lyapunov function-based parameter adaptive law and the strictly proven control system stability. Because of the advantages of the nonlinear adaptive fuzzy control, it has been used in the control of power converters and motors recently. In [16], direct adaptive fuzzy control is used to control a reluctance motor, the controller has good dynamic performance versus stator resistance. In [17], an indirect adaptive fuzzy controller is proposed for a class of switching power converters which subject to external disturbances. In [18], a direct adaptive fuzzy controller is designed to control the speed of a permanent magnet synchronous motor.

In this paper, a nonlinear direct adaptive fuzzy controller is proposed to stabilize both the L- and LCL-based single-phase three-level grid-connected inverters. Section 2 introduces the inverter topology and its pulse-width modulation method. Section 3 describes the theory of the adaptive fuzzy control and gives the design process of the controller for the inverters. The performance of the control scheme is evaluated through simulations, and the results are shown in Section 4.

2 Principle of single-phase three-level grid-connected inverter

Fig. 1 shows the topology of the single-phase three-level grid-connected inverter [2]. The dc voltage is denoted as u_{dc}. The two split capacitors (C_1 and C_2) have equal voltages, that is $u_{C1} = u_{C2} = u_{dc}/2$. The inverter has two legs, each has four switches and two diodes, which constitute a classical neutral-point-clamped (NPC) topology. The inverter can be connected to the grid through a single inductor (L_{g1}) or an LCL filter (L_i, L_{g2}, C_g). The grid voltage and the grid-connected current are denoted as u_g and i_g respectively.

DOI: 10.1587/elex.15.20180838
Received September 3, 2018
Accepted November 6, 2018
Publicized November 16, 2018
Copyedited December 10, 2018

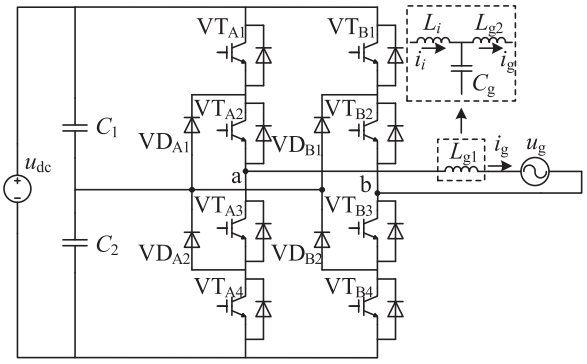

Fig. 1. Topology of a single-phase three-level grid-connected inverter

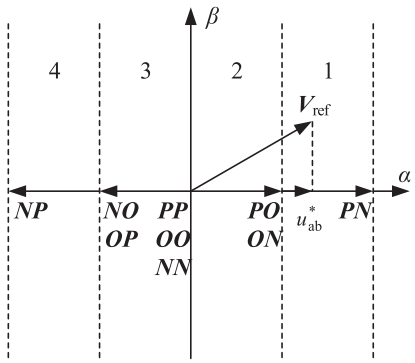

Fig. 2. Space voltage vector diagram for single-phase three-level inverter

Fig. 2 shows the space vector diagram for a single-phase three-level inverter. The $\alpha\beta$ plane is divided into 4 sections. The reference voltage $\boldsymbol{V}_{\text{ref}}$ rotates anticlockwise in the plane with angular velocity ω and passes through sections $1 \rightarrow 2 \rightarrow 3 \rightarrow 4 \rightarrow 4 \rightarrow 3 \rightarrow 2 \rightarrow 1$ in sequence. The reference output voltage of the inverter is denoted as u^*_{ab}, which is a projection of $\boldsymbol{V}_{\text{ref}}$ on α-axis. A criterion is employed to determine the location of u^*_{ab}:

(1) Section 1: $0.5 < u^*_{\text{ab}}/u_{\text{dc}} \leq 1$.
(2) Section 2: $0 < u^*_{\text{ab}}/u_{\text{dc}} \leq 0.5$.
(3) Section 3: $-0.5 < u^*_{\text{ab}}/u_{\text{dc}} \leq 0$.
(4) Section 4: $-1 \leq u^*_{\text{ab}}/u_{\text{dc}} \leq -0.5$.

The reference voltage can be synthesized by the nearest standard voltage vectors. If $\boldsymbol{V}_{\text{ref}}$ is located in Section 1, it is synthesized by vectors ***PO***(***ON***) and ***PN***. If $\boldsymbol{V}_{\text{ref}}$ is located in Section 2, it is synthesized by vectors ***PO***(***ON***) and ***OO***(***PP***, ***NN***). If $\boldsymbol{V}_{\text{ref}}$ is located in Section 3, it is synthesized by vectors ***OP***(***NO***) and ***OO***(***PP***, ***NN***). If $\boldsymbol{V}_{\text{ref}}$ is located in Section 4, it is synthesized by vectors ***OP***(***NO***) and ***NP***.

A five-segment optimal SVPWM method is used in this paper to reduce the switching frequency and the switching losses. Table I shows the output voltage vectors operation sequence in each section. In one switching period, only two switches in each bridge change their states. For example, in Section 1, switches VT_{A1} and VT_{A3} in leg A turn on once and turn off once, and so do switches VT_{B2} and VT_{B4} in leg B, which is illustrated in Fig. 3.

DOI: 10.1587/elex.15.20180838
Received September 3, 2018
Accepted November 6, 2018
Publicized November 16, 2018
Copyedited December 10, 2018

Table I. Output voltage vectors operation sequence

Section	Vectors operation sequence
1	***PO*** → ***PN*** → ***ON*** → ***PN*** → ***PO***
2	***PO*** → ***OO*** → ***ON*** → ***OO*** → ***PO***
3	***OP*** → ***OO*** → ***NO*** → ***OO*** → ***OP***
4	***OP*** → ***NP*** → ***NO*** → ***NP*** → ***OP***

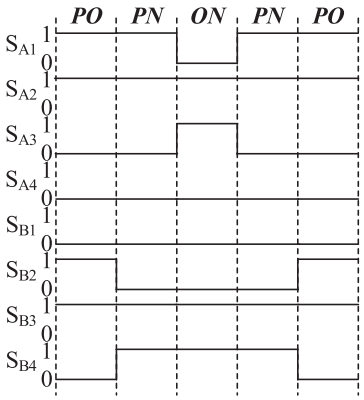

Fig. 3. Sequence diagram of output voltage vectors (Section 1)

By the principle of volt-second balance, the duty times of vectors in each switching period can be obtained by (1), the results are shown in Table II.

$$\begin{cases} V_1 t_1 + V_2 t_2 = u_{ab}^* T_s \\ t_1 + t_2 = T_s \end{cases} \tag{1}$$

Table II. Duty time of output voltage vectors

Section	t_1	t_2
1	$2(u_{dc} - u_{ab}^*)T_s/u_{dc}$	$(2u_{ab}^* - u_{dc})T_s/u_{dc}$
2	$2u_{ab}^* T_s/u_{dc}$	$(u_{dc} - 2u_{ab}^*)T_s/u_{dc}$
3	$-2u_{ab}^* T_s/u_{dc}$	$(u_{dc} + 2u_{ab}^*)T_s/u_{dc}$
4	$2(u_{dc} + u_{ab}^*)T_s/u_{dc}$	$-(u_{dc} + 2u_{ab}^*)T_s/u_{dc}$

3 Nonlinear direct adaptive fuzzy control

In this section, we first explain the nonlinear direct adaptive control based on literatures [10, 11, 12, 13, 14, 15], and then show how to develop a direct adaptive fuzzy controller for the two types of grid-connected inverters.

3.1 Direct adaptive fuzzy control

Consider the nonlinear systems of the form

$$\begin{cases} x^{(n)} = f(x, \dot{x}, \cdots x^{(n-1)}) + bu \\ y = x \end{cases} \tag{2}$$

where f is a continuous unknown function, b is a positive unknown constant, $u \in R$ and $y \in R$ are the input and output of the system, respectively. It assumed that the state vector $\boldsymbol{x} = (x, \dot{x}, \cdots x^{(n-1)})^{\mathrm{T}}$ is measurable.

DOI: 10.1587/elex.15.20180838
Received September 3, 2018
Accepted November 6, 2018
Publicized November 16, 2018
Copyedited December 10, 2018

Control objectives. Determine a feedback control $u(\boldsymbol{x}|\boldsymbol{\theta})$ and an adaptive law for adjusting the parameter vector $\boldsymbol{\theta}$ such that:

1) The closed-loop system is globally stable with all the variables are uniformly bounded.

2) For a given bounded reference signal y_{m}, the tracking error $e = y_{\mathrm{m}} - y$ converges to a value as small as possible.

The adaptive fuzzy control law is the sum of basic control $u_c(\boldsymbol{x}|\boldsymbol{\theta})$ and the supervisory control $u_{\mathrm{s}}(\boldsymbol{x})$:

$$u = u_{\mathrm{c}}(\boldsymbol{x}|\boldsymbol{\theta}) + u_{\mathrm{s}}(\boldsymbol{x}) \tag{3}$$

where $u_{\mathrm{c}}(\boldsymbol{x}|\boldsymbol{\theta})$ is a fuzzy logic system. Substituting (3) into (2), we have

$$x^{(n)} = f(\boldsymbol{x}) + b[u_{\mathrm{c}}(\boldsymbol{x}|\boldsymbol{\theta}) + u_{\mathrm{s}}(\boldsymbol{x})] \tag{4}$$

If $f(\boldsymbol{x})$ and b are known, then the control law

$$u^* = \frac{1}{b}[-f(\boldsymbol{x}) + y_{\mathrm{m}}^{(n)} + \boldsymbol{k}^{\mathrm{T}}\boldsymbol{e}] \tag{5}$$

will force the error e converge to zero. In (5), $\boldsymbol{e} = (e, \dot{e}, \cdots, e^{(n-1)})^{\mathrm{T}}$ and $\boldsymbol{k} = (k_{\mathrm{n}}, \cdots, k_1)^{\mathrm{T}}$ make all roots of $s^{\mathrm{n}} + k_1 s^{\mathrm{n}-1} + \cdots + k_{\mathrm{n}} = 0$ are in the open left-half plane. Adding and subtracting bu^* to (4) we obtain the error equation of the closed-loop system:

$$e^{(n)} = -\boldsymbol{k}^{\mathrm{T}}\boldsymbol{e} + b[u^* - u_{\mathrm{c}}(\boldsymbol{x}|\boldsymbol{\theta}) - u_{\mathrm{s}}(\boldsymbol{x})] \tag{6}$$

or equivalently,

$$\dot{\boldsymbol{e}} = \boldsymbol{\Lambda}_{\mathrm{c}}\boldsymbol{e} + \boldsymbol{b}_{\mathrm{c}}[u^* - u_{\mathrm{c}}(\boldsymbol{x}|\boldsymbol{\theta}) - u_{\mathrm{s}}(\boldsymbol{x})] \tag{7}$$

where

$$\boldsymbol{\Lambda}_{\mathrm{c}} = \begin{bmatrix} 0 & 1 & 0 & 0 & \cdots & 0 & 0 \\ 0 & 0 & 1 & 0 & \cdots & 0 & 0 \\ \vdots & \vdots & \vdots & \vdots & \vdots & \vdots & \vdots \\ 0 & 0 & 0 & 0 & 0 & 0 & 1 \\ -k_n & -k_{n-1} & -k_{n-2} & -k_{n-3} & \cdots & -k_2 & -k_1 \end{bmatrix}, \quad \boldsymbol{b}_{\mathrm{c}} = \begin{bmatrix} b \\ \vdots \\ 0 \\ 1 \end{bmatrix}$$

Define $V_{\mathrm{c}} = \frac{1}{2}\boldsymbol{e}^{\mathrm{T}}\boldsymbol{P}\boldsymbol{e}$, where $\boldsymbol{P}$ is a symmetric positive definite matrix satisfying the Lyapunov equation

$$\boldsymbol{\Lambda}_{\mathrm{c}}^{\mathrm{T}}\boldsymbol{P} + \boldsymbol{P}\boldsymbol{\Lambda}_{\mathrm{c}} = -\boldsymbol{Q} \tag{8}$$

where $\boldsymbol{Q}$ is an arbitrary $n \times n$ positive definite matrix. From (7) and (8) we have

$$\begin{aligned} \dot{V}_{\mathrm{c}} &= \frac{1}{2}\dot{\boldsymbol{e}}^{\mathrm{T}}\boldsymbol{P}\boldsymbol{e} + \frac{1}{2}\boldsymbol{e}^{\mathrm{T}}\boldsymbol{P}\dot{\boldsymbol{e}} = -\frac{1}{2}\boldsymbol{e}^{\mathrm{T}}\boldsymbol{Q}\boldsymbol{e} + \boldsymbol{e}^{\mathrm{T}}\boldsymbol{P}\boldsymbol{b}_{\mathrm{c}}[u^* - u_{\mathrm{c}}(\boldsymbol{x}|\boldsymbol{\theta}) - u_{\mathrm{s}}(\boldsymbol{x})] \\ &\leq -\frac{1}{2}\boldsymbol{e}^{\mathrm{T}}\boldsymbol{Q}\boldsymbol{e} + |\boldsymbol{e}^{\mathrm{T}}\boldsymbol{P}\boldsymbol{b}_{\mathrm{c}}|(|u^*| + |u_{\mathrm{c}}|) - \boldsymbol{e}^{\mathrm{T}}\boldsymbol{P}\boldsymbol{b}_{\mathrm{c}}u_{\mathrm{s}} \end{aligned} \tag{9}$$

We construct the supervisory control $u_{\mathrm{s}}(\boldsymbol{x})$ as follows:

$$u_{\mathrm{s}}(\boldsymbol{x}) = I_1^* \operatorname{sgn}(\boldsymbol{e}^{\mathrm{T}}\boldsymbol{P}\boldsymbol{b}_{\mathrm{c}})\left[|u_{\mathrm{c}}| + \frac{1}{b_{\mathrm{L}}}(f^{\mathrm{U}} + |y_{\mathrm{m}}^{(n)}| + |\boldsymbol{k}^{\mathrm{T}}\boldsymbol{e}|)\right] \tag{10}$$

DOI: 10.1587/elex.15.20180838
Received September 3, 2018
Accepted November 6, 2018
Publicized November 16, 2018
Copyedited December 10, 2018

where b_L is a constant, $0 \le b_L \le b$; f^U is the upper bound of $f(x)$; $I_1^* = 1$ if $V_c \ge \bar{V}$ ($\bar{V}$ is a constant specified by the designer) and $I_1^* = 0$ if $V_c \le \bar{V}$. Substitute (10) to (9) and considering the $I_1^* = 1$ case, we have

$$\begin{aligned}\dot{V}_c &\le -\frac{1}{2}\boldsymbol{e}^T\boldsymbol{Q}\boldsymbol{e} + |\boldsymbol{e}^T\boldsymbol{P}\boldsymbol{b}_c|\left[\frac{1}{b}(|f| + |y_m^{(n)}| + |\boldsymbol{k}^T\boldsymbol{e}|)\right.\\ &\quad \left. + |u_c| - |u_c| - \frac{1}{b_L}(|f^U| + |y_m^{(n)}| + |\boldsymbol{k}^T\boldsymbol{e}|)\right]\\ &\le -\frac{1}{2}\boldsymbol{e}^T\boldsymbol{Q}\boldsymbol{e} \le 0\end{aligned} \tag{11}$$

So if we use the supervisory control u_s in (10), we always have $V_c \le \bar{V}$.

Define the optimal parameter vector

$$\theta^* = \arg\min_{|\theta|\le M_\theta}[\sup_{|x|\le M_x}|u_c(\boldsymbol{x}|\boldsymbol{\theta}) - u^*|] \tag{12}$$

and the minimum fuzzy approximation error

$$\omega = u_c(\boldsymbol{x}|\boldsymbol{\theta}) - u^* \tag{13}$$

Take the parameter adaptive law as

$$\dot{\boldsymbol{\theta}} = \gamma\boldsymbol{e}^T\boldsymbol{P}\boldsymbol{b}_c \tag{14}$$

To guarantee $|\boldsymbol{\theta}| \leqslant M_\theta$, the adaptive law in (14) is corrected as

$$\dot{\boldsymbol{\theta}} = \begin{cases} \gamma\boldsymbol{e}^T\boldsymbol{p}_n\boldsymbol{\xi}(\boldsymbol{x}) & \text{if } |\boldsymbol{\theta}| < M_\theta \\ & \text{or } |\boldsymbol{\theta}| = M_\theta \text{ and } \boldsymbol{e}^T\boldsymbol{p}_n\boldsymbol{\theta}^T\boldsymbol{\xi}(\boldsymbol{x}) \le 0 \\ P_r[\gamma\boldsymbol{e}^T\boldsymbol{p}_n\boldsymbol{\xi}(\boldsymbol{x})] & \text{if } |\boldsymbol{\theta}| = M_\theta \text{ and } \boldsymbol{e}^T\boldsymbol{p}_n\boldsymbol{\theta}^T\boldsymbol{\xi}(\boldsymbol{x}) \ge 0 \end{cases} \tag{15}$$

where $P_r[\cdot]$ is the projection operator defined as

$$P_r[\gamma\boldsymbol{e}^T\boldsymbol{p}_n\boldsymbol{\xi}(\boldsymbol{x})] = \gamma\boldsymbol{e}^T\boldsymbol{p}_n\boldsymbol{\xi}(\boldsymbol{x}) - \gamma\boldsymbol{e}^T\boldsymbol{p}_n\frac{\boldsymbol{\theta}\boldsymbol{\theta}^T\boldsymbol{\xi}(\boldsymbol{x})}{|\boldsymbol{\theta}|^2} \tag{16}$$

where $\gamma > 0$ is the learning law and $\boldsymbol{p}_n$ is the last column of matrix $\boldsymbol{P}$.

The direct adaptive fuzzy control has three design steps:

Step 1. Off-line preprocessing.

1) Specify a set of parameters $k_1, \cdots, k_n$ such that all roots of $s^n + k_1 s^{n-1} + \cdots + k_n = 0$ are in the open left-half plane.

2) Specify a positive definite matrix $\boldsymbol{Q}$, solve the Lyapunov equation (8), to obtain a positive definite matrix $\boldsymbol{P}$.

3) Specify the design parameter M_θ based on practical constraints.

Step 2. Construct fuzzy controller.

1) Construct the fuzzy rule base which consists of the rules

R^i: IF x_1 is F_1^i and x_2 is F_2^i and $\cdots$ and x_n is F_n^i,

THEN u_c is B_i; $i = 1, 2, \cdots, N$

2) Construct the fuzzy basis functions

$$\xi_i(x_1, \cdots, x_n) = \frac{\prod_{j=1}^{n}\mu_{F_j^i}(x_j)}{\sum_{i=1}^{N}\left(\prod_{j=1}^{n}\mu_{F_j^i}(x_j)\right)} \tag{17}$$

DOI: 10.1587/elex.15.20180838
Received September 3, 2018
Accepted November 6, 2018
Publicized November 16, 2018
Copyedited December 10, 2018

where $\mu_F(x)$ is the membership function. Make an N-dimensional vector $\boldsymbol{\xi}(\boldsymbol{x}) = [\xi_1, \cdots, \xi_N]^{\mathrm{T}}$ and the $u_{\mathrm{c}}(\boldsymbol{x}|\boldsymbol{\theta})$ is constructed as

$$u_{\mathrm{c}}(\boldsymbol{x}|\boldsymbol{\theta}) = \sum_{i=1}^{N} \theta_i \xi(\boldsymbol{x}) = \boldsymbol{\theta}^{\mathrm{T}} \boldsymbol{\xi}(\boldsymbol{x}) \tag{18}$$

Step 3. On-line adaption.

1) Apply the feedback control (3) to the plant (2), where u_{c} is given by (18) and u_{s} is given by (10).

2) Use (15) and (16) to adjust the parameter $\boldsymbol{\theta}$.

3.2 Controller design for the single-phase three-level grid-connected inverter

The state variable $x(t)$ is chosen as the current of L_{g1} (i_{g}) and the current of L_i (i_i) for L-based and LCL-based grid-connected inverters respectively, and u_{ab} can be denoted as u, so both grid-connected inverters can be expressed by state equation in (19).

$$\dot{x} = \frac{u}{L} - \frac{u_{\mathrm{g}}}{L} \tag{19}$$

where $L = L_{\mathrm{g1}}$ and $L = L_i$ for L-based and LCL-based grid-connected inverters respectively.

In a specific application, the amplitude of the grid-connected current is always less than 50 A, and the gain of the measurement circuit is supposed as 1/10. So we define six fuzzy sets over the interval $[-5, 5]$, with labels N_3, N_2, N_1, P_1, P_2, P_3, and membership functions $\mu_{N3} = 1/(1 + \exp(-5(x + 4)))$, $\mu_{N2} = \exp(-(x + 3)^2)$, $\mu_{N1} = \exp(-(x + 2)^2)$, $\mu_{P1} = \exp(-(x - 2)^2)$, $\mu_{P2} = \exp(-(x - 3)^2)$, $\mu_{P3} = 1/(1 + \exp(-5(x - 4)))$. The learning law $\gamma = 1$ and $\boldsymbol{p}_n = [4000000]$ ($n = 1$). Not that the supervisory control is not involved ($I_1^* = 0$) because although it can force the grid-connected current back to the constraint set, it also leads to current distortion (The current will be chopped). Therefore, a maximum amplitude of about 20~30 A is recommended in this specific application such that the state will not hit the boundary.

The control block diagram of the adaptive fuzzy controller is shown in Fig. 4.

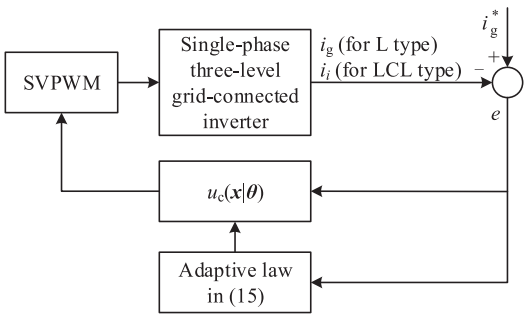

Fig. 4. Control block diagram of the adaptive fuzzy controller

DOI: 10.1587/elex.15.20180838
Received September 3, 2018
Accepted November 6, 2018
Publicized November 16, 2018
Copyedited December 10, 2018

4 Simulation studies

The proposed nonlinear direct adaptive fuzzy controller for the L- and LCL-based grid-connected inverters is verified under MATLAB/Simulink environment. The dc side voltage is $u_{dc} = 200$ V. The rms value of the grid voltage is $U_g = 220$ V. The switching frequency is $f_s = 10$ kHz.

The results for the L-based grid-connected inverter are shown in Fig. 5. The amplitude of reference grid-connected current is 10 A, and changes to 20 A at $t = 0.105$ s. Fig. 4(a)~(c) are the results for case 1, in which $L_{g1} = 3$ mH. Fig. 4(a) illustrates that the grid-connected current i_g is sinusoidal and in phase with the grid voltage u_g. Note that i_g is magnified 5 times in Fig. 5(a) to give a clearer view. From Fig. 5(b), we can see the five-level inverter output voltage with peak value of 500 V. Fig. 5(c) shows i_g without magnification, we can see that its steady state amplitude is 10 A before $t = 0.105$ s and changes to 20 A after that instant. The steady state errors before and after $t = 0.105$ s are both close to zero. The transient process is very short and the overshoot is also very small, the transient peak value is about 23.5 A. Fig. 5(d)~(e) illustrate i_g for case 2 and case 3, in which L_{g1} are 5 mH and 10 mH respectively. It can be seen that the system is still stable even when the inductance changes significantly. The transient peak values increase compared to case 1, which are about 24.5 A in case 2 and 26.5 A in case 3.

Then, the controller for L-based grid-connected inverter is used to control the LCL-based grid-connected inverter without any modification. The current of L_i (i_i)

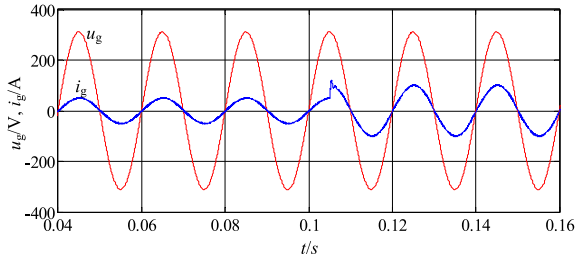

(a) Grid voltage and grid-connected current (Case 1: L_{g1}=3mH)

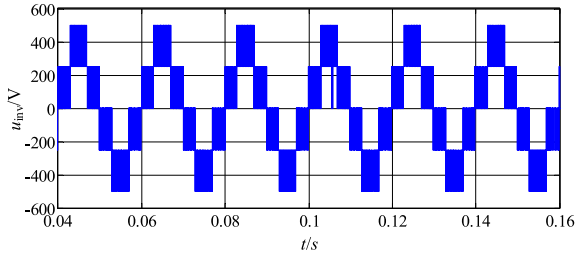

(b) Inverter output voltage (Case 1: L_{g1}=3mH)

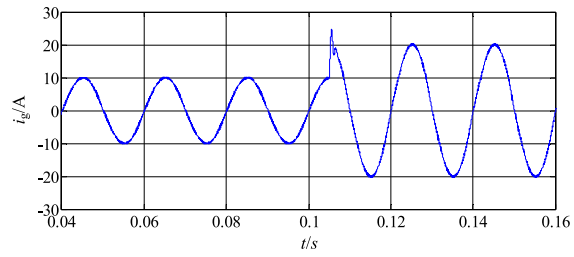

(c) Grid-connected current (Case 1: L_{g1}=3mH)

DOI: 10.1587/elex.15.20180838
Received September 3, 2018
Accepted November 6, 2018
Publicized November 16, 2018
Copyedited December 10, 2018

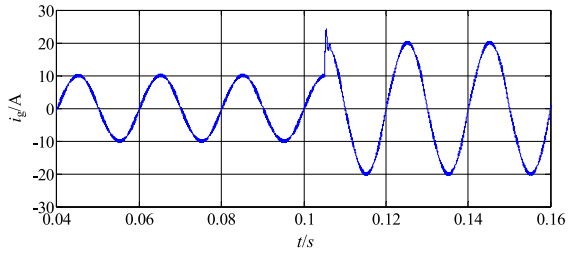

(d) Grid-connected current (Case 2: L_{g1}=5mH)

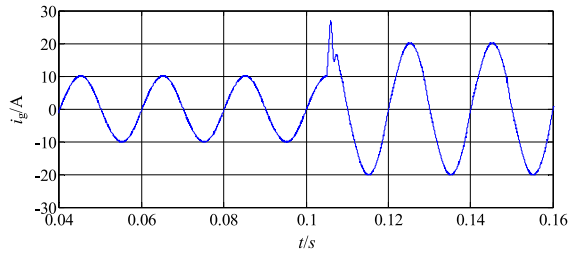

(e) Grid-connected current (Case 3: L_{g1}=10mH)

Fig. 5. Simulation results for L-based grid-connected inverter

is taken as the feedback signal. The results are shown in Fig. 6. Fig. 6(a)~(c) are the results for case 4, in which $L_i = 1$ mH, $L_{g2} = 0.5$ mH and $C_g = 2$ μF. It is clear that the controller is also effective in stabilizing the LCL filter. It is shown in Fig. 6(a) that i_g has lower harmonics compared to case 1 even the sum of L_i and L_{g2} (1 mH + 0.5 mH) is smaller than L_{g1} in case 1 (3 mH). Better filtering effect is achieved, which is the most outstanding advantage of an LCL filter. Fig. 6(d)~(e) illustrate i_g for case 5 and case 6, in which $L_i = 1$ mH, $L_{g2} = 0.5$ mH, $C_g = 2$ μF and $L_i = 4$ mH, $L_{g2} = 2$ mH, $C_g = 10$ μF respectively. The system is still stable but the transient peak values increase compared to case 4, which are about 24.5 A in case 5 and 29.5 A in case 6. Fig. 6(f) shows the six fuzzy basis functions, which change obviously after $t = 0.105$ s. Fig. 6(g) shows the track error of i_g in case 5.

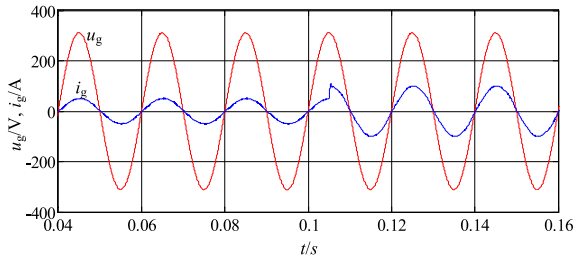

(a) Grid voltage and grid-connected current (Case 4: L_i=1mH, L_{g2}=0.5mH, C_g=2μF)

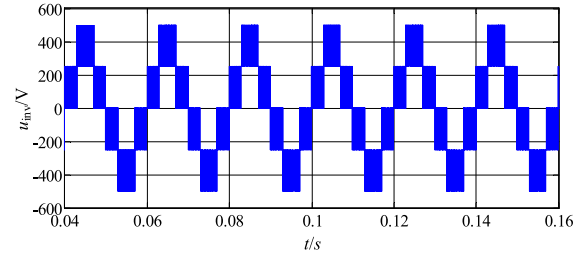

(b) Inverter output voltage (Case 4: L_i=1mH, L_{g2}=0.5mH, C_g=2μF)

DOI: 10.1587/elex.15.20180838
Received September 3, 2018
Accepted November 6, 2018
Publicized November 16, 2018
Copyedited December 10, 2018

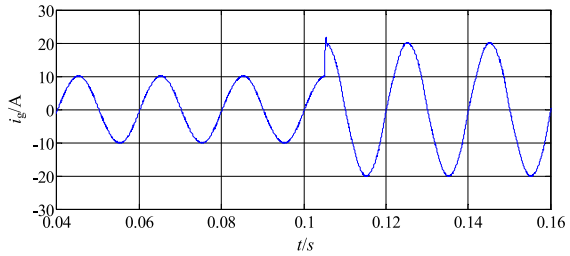

(c) Grid-connected current (Case 4: L_i=1mH, L_{g2}=0.5mH, C_g=2μF)

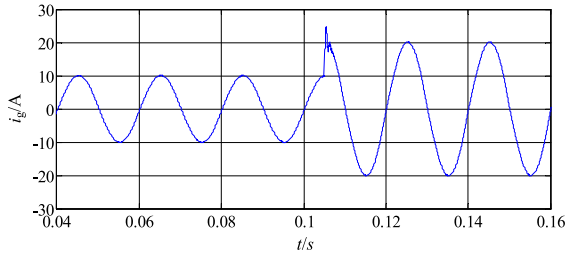

(d) Grid-connected current (Case 5: L_i=2.5mH, L_{g2}=0.5mH, C_g=3μF)

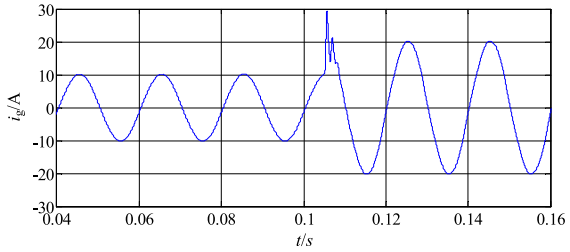

(e) Grid-connected current (Case 6: L_i=4mH, L_{g2}=2mH, C_g=10μF)

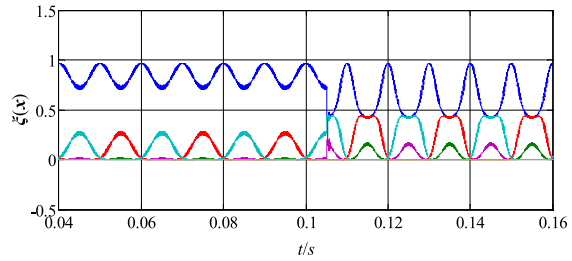

(f) Fuzzy basis functions (Case 5: L_i=2.5mH, L_{g2}=0.5mH, C_g=3μF)

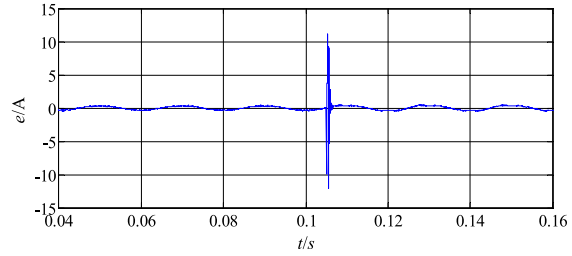

(g) Tracking error (Case 5: L_i=2.5mH, L_{g2}=0.5mH, C_g=3μF)

Fig. 6. Simulation results for LCL-based grid-connected inverter

The transient error is relatively large (greater than ±10 A) while the transient peak value is only about 24.5 A, which can be seen in Fig. 6(d) (the transient error should $24.5 - 20 = 4.5$ A). The reason is that the error in Fig. 6(g) is actually $i_i^* - i_g$ while there is a phase difference between the two currents.

DOI: 10.1587/elex.15.20180838
Received September 3, 2018
Accepted November 6, 2018
Publicized November 16, 2018
Copyedited December 10, 2018

5 Conclusions

In this paper, a nonlinear direct adaptive fuzzy control method is proposed to control both the L- and LCL-based grid-connected inverters. The adaptive fuzzy control provides an easy way to design the control system and the controller is not sensitive to system parameters and disturbances. The stability of the closed-loop system can be strictly proved. The simulation results show that the two types of grid-connected inverters work stably when the values of inductance and capacitance vary within large ranges and the controller has strong robustness. For future work, other adaptive fuzzy control methods such as adaptive sliding mode fuzzy control and adaptive output feedback fuzzy control for the grid-connected inverters will be studied.

Acknowledgments

This work was supported by the “Guangzhou Science and Technology Planning Project of China”, no. 201607010262 and the “Guangdong Provincial Science and Technology Planning Project of China”, no. 2015A010106015.

DOI: 10.1587/elex.15.20180838
Received September 3, 2018
Accepted November 6, 2018
Publicized November 16, 2018
Copyedited December 10, 2018